Ultrastructure of Skeletal Muscle Fibers Studied by a Plunge Quick Freezing Method: Myofilament Lengths

Hernando Sosa, David Popp, Greta Ouyang, and Hugh E. Huxley
Rosenstiel Center and Department of Biology, Brandeis University, Waltham, Massachussetts 02254 USA

ABSTRACT We have set up a system to rapidly freeze muscle fibers during contraction to investigate by electron microscopy the ultrastructure of active muscles. Glycerinated fiber bundles of rabbit psoas muscles were frozen in conditions of rigor, relaxation, isometric contraction, and active shortening. Freezing was carried out by plunging the bundles into liquid ethane. The frozen bundles were then freeze-substituted, plastic-embedded, and sectioned for electron microscopic observation. X-ray diffraction patterns of the embedded bundles and optical diffraction patterns of the micrographs resemble the x-ray diffraction patterns of unfixed muscles, showing the ability of the method to preserve the muscle ultrastructure. In the optical diffraction patterns layer lines up to 1/5.9 nm^{-1} were observed. Using this method we have investigated the myofilament lengths and concluded that there are no major changes in length in either the actin or the myosin filaments under any of the conditions explored.

INTRODUCTION

Observations by optical microscopy of skeletal muscle fibers (Huxley and Niedegerke, 1954) and isolated myofibrils (Huxley and Hanson, 1954) led to the sliding filament model of muscle contraction. According to this model, muscle contraction is the result of a sliding force between the actin and myosin filaments. This force is created by cross-bridges connecting the two sets of filaments without requiring length changes in the filaments themselves. Although there is still little direct evidence about the structural change in the cross-bridges responsible for contraction, this model is consistent with most of the experimental data and is widely accepted.

Despite the acceptance of the sliding filament model, a common observation in the optical microscope is that at sarcomere lengths below the resting length the A-band seems shorter (Huxley and Niedegerke, 1954, 1958; Huxley and Hanson, 1954). This phenomenon has been attributed to limits in the resolution of the optical microscope (Huxley and Niedegerke, 1958). Higher resolution electron microscope (EM) studies using conventional specimen fixation methods have shown that the length of the filaments remains unchanged between resting and contraction at sarcomere lengths greater than 2.1 μm (Page and Huxley, 1963). But some other EM studies (reviewed by Pollack, 1983, 1990) have reported variation in filament length. Most cases of reported filament length changes in electron microscope studies have previously been attributed to several kinds of artifacts (Page and Huxley, 1963; Huxley, 1985). (An exceptional case seems to occur in *Limulus* striated muscle, in which shortening of the A band has consistently been reported, but it has been attributed to fragmentation and depolymerization at the ends of the filaments, and not to homogeneous shortening (De Villafranca, 1961; Dewey et al., 1973; Levine et al., 1991).) In a more recent study using optical microscopy with improved optics and electron microscopy, it was reported that A-band shortening as high as 50% took place in vertebrate muscle fibers during active shortening (Periasamy et al., 1990). This uncertainty about the length of the filaments under certain conditions has left open the possibility of models in which myofilament shortening plays a role in the molecular mechanism of muscle contraction (e.g., Pollack, 1983, 1990; Schutt and Lindberg, 1992). Therefore, additional evidence about the length of the myofilaments during contraction is desirable.

Electron microscopy, in contrast to optical microscopy, provides sufficient resolution to measure the myofilaments length accurately, but the use of chemical fixation, as in conventional procedures, is open to criticism on the ground that it is too slow (seconds) to capture fast dynamic processes like the ones occurring during muscle contraction. Rapid freezing techniques, however, offer an alternative method for preparing specimens for the electron microscope that, in principle, is able to trap processes occurring in a time scale of milliseconds (Heuser et al., 1979; Jones, 1984). For this reason and because very good ultrastructural preservation is achieved, rapid freezing is being applied increasingly in muscle studies.

Two methods that have been used to rapidly freeze muscle samples are the slamming method (e.g., Van Harreveld et al., 1974; Heuser et al., 1979; Tsukita and Yano, 1985; Huxley, 1987; Hirose and Wakabayashi, 1988; Padrón et al., 1988, 1992; Padrón and Craig, 1989; Craig et al., 1992; Hirose et al., 1993) and the plunging one (e.g., McDowall et al., 1984; Trus et al., 1989). In the slamming method the sample is frozen by contact (slamming) against a cold metal block, whereas in the plunging method the sample is frozen by plunging it into a liquid cryogen. It is estimated that the

Received for publication 4 February 1994 and in final form 28 March 1994.
Address reprint requests to Hugh E. Huxley, Rosentiel Basic Medical Sciences Research Center, Brandeis University, 415 South Street, Waltham, MA 02254-9110. Tel.: 617-736-2490; Fax: 617-736-2405.

0006-3495/94/07/283/10 $2.00

cooling rate for the slamming method is higher than for the plunging one (Bald, 1985), but with both methods it is possible to achieve cooling rates high enough to avoid ice crystal damage up to a specimen depth of several microns (see Elder et al., 1982; Jones, 1984).

In this paper we report the development of a plunge freezing and freeze substitution method for muscle fibers that gives improved structural preservation and allows mechanical manipulation of the fibers while freezing. We chose a plunge freezing technique for its relative simplicity and reduced mechanical stress to the sample at the moment of freezing. In addition, as shown in this paper, the use of cryoprotectants makes it possible to obtain muscle fibers that are uniformly well preserved and are suitable for x-ray diffraction.

We have used this method to measure by electron microscopy the myofilaments lengths in conditions of relaxation, rigor, isometric contraction, and active shortening. Some of the results have been presented in preliminary form (Sosa et al., 1992).

MATERIALS AND METHODS

Solutions

Solution A: 100 mM potassium propionate, 3 mM $MgCl_2$, 10 mM Imidazole, pH = 7.0. Skinning: 70 mM potassium propionate, 8 mM magnesium acetate, 5 mM EGTA, 7 mM ATP, 6 mM Imidazole, 0.1 mM phenylmethylsulfonylfluoride (PMSF), pH = 7.0. Storage: the same as the skinning solution but diluted with glycerol 50% v/v and including 10 mM glutathione, 5 mM NaN_3. Relaxing: 5.4 mM ATP, 7.4 mM $MgCl_2$, 30 mM EGTA, 100 mM *N*-tris[hydroxymethyl]-methyl-2-aminoethane-sulfonic acid (TES), pH = 7.0. Pre-activation: 5.4 mM ATP, 7.4 mM $MgCl_2$, 0.1 mM EGTA, 22 mM phosphocreatine, 1 mg/ml creatine-phosphokinase (Type I, Sigma, St Louis, MO, USA), 100 mM TES, pH = 7.0. Activating: 5.4 mM ATP, 7.4 mM $MgCl_2$, 30 mM EGTA, 30 mM $CaCl_2$, 22 mM phosphocreatine, 1 mg/ml creatine-phosphokinase, 100 mM TES, pH = 7.0.

For freezing, cryoprotectant was added to the appropriate solutions, 15% (v/v) glycerol, 15% (v/v) propylene glycol, or 15% (w/v) glucose. Any of these three cryoprotectants gave good results, although some of the best micrographs were obtained with propylene glycol and with glucose.

Muscle fibers

Chemically skinned rabbit psoas muscle fiber bundles were obtained by the method of Eastwood et al. (1979). Strips of psoas muscle ~85 mm long and ~5 mm wide were dissected from New Zealand white rabbits (Pine Acre rabbitry, Norton, MA) and tied to plastic sticks at rest length or stretched about 30%. The muscle strips were placed in the rabbit skinning solution for 48 h at 4°C with one solution exchange. The bundles were then transferred to the storage solution for 24 h at 4°C and then stored at −20°C in fresh storage solution for at least 1 week before use.

Experimental setup

Fig. 1 shows a scheme of the apparatus used for mechanical experiments and rapid freezing. Fiber bundles 5–10 mm long were glued with cyanoacrylate glue (Krazy Glue, Borden Inc., Columbus, OH) at one end to a force transducer (model KG3, Scientific Instruments GMBH, Heidelberg, Germany) and at the other end to a motor driven lever (model 305, Cambridge Technology Inc. Watertown, MA). The lever system and the transducer were mounted on a pneumatic mechanism that plunges the fibers rapidly into the cryogen. In this system the fiber bundle is accelerated to a speed of 2.3 m/s before crossing the cryogen-air interface and then travels 15 mm into the cryogen before being stopped. A movable solution receptacle was used to keep the bundles in the appropriate solution up to the moment of plunging. After the solution receptacle was withdrawn, the fiber bundle remained in air ~1 s until plunged into the cryogen. The position of the lever motor was controlled with a waveform generator (model 75, Wavetek, San Diego, CA). A pair of infrared optical switches (part 105–20, HEI Inc., Victoria, MN) was used to synchronize the length changes with the plunging event. Muscle tension and the lever position was recorded on a digital oscilloscope (model 2221, Tektronix Inc., Beaverton, OR) and transferred to an IBM-compatible personal computer for storage and later analysis using custom written software. To measure the sarcomere length before freezing, a laser beam (model 134, Spectra Physics, Mountain View, CA) was routed through the fiber bundle and projected on a calibrated screen.

The cryogen (liquid ethane) was contained in a special device made out of Teflon (E.I. DuPont de Nemours, Wilmington, DE) based on the design by Robards et al. (1988). This device consists of a cryogen reservoir with a central compartment. A magnetic stirrer makes the cryogen flow continuously upward in the central compartment to overflow into the reservoir. The sample is plunged into the central compartment in which the cryogen overflows at a constant height, so we could adjust very precisely the time point in which the sample crosses the air-cryogen interface. With this device we could keep liquid ethane flowing without freezing at a temperature between −175 and −180°C for a whole experimental session (1–4 h).

Experimental protocol

Fiber bundles of rabbit psoas muscles were rapidly frozen in relaxing, rigor, or contracting conditions. Contracting muscles were frozen either in isometric conditions or during active shortening. Relaxing condition: the bundles were transferred from the storage solution to the relaxing solution and frozen. Rigor condition: the bundles were transferred from the relaxing solution to the solution A and frozen after rigor tension reached a plateau.

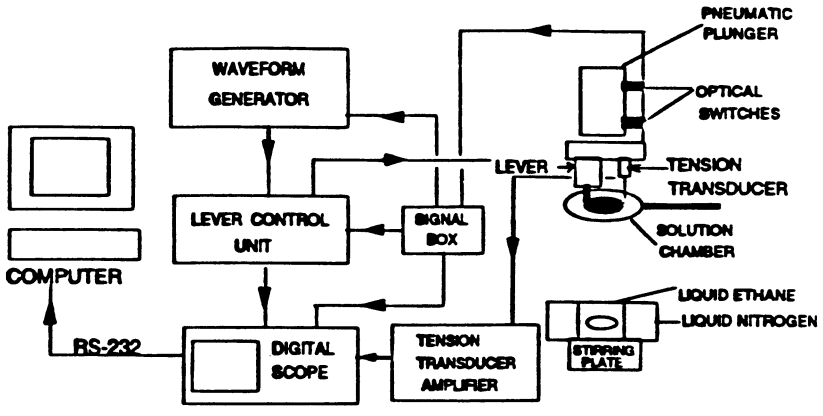

FIGURE 1 Experimental set-up used for rapid freezing and mechanical experiments on muscle fibers.

Alternatively, the bundles were transferred from the storage solution to the solution A with 50% glycerol, kept overnight at −20°C, and then transferred to the solution A and frozen. Contracting conditions: bundles were transferred from the relaxing solution to the pre-activating solution (Moisescu, 1976) and then to the activating solution, where they would develop tension (maximum isometric tension was ~27 Nt/cm^2 without cryoprotectants and ~20% less in its presence). After active tension reached a plateau, typically 2 to 6 s after the solution change, the bundle was either allowed to shorten and frozen during shortening (active shortening condition) or frozen, keeping the bundle length constant (isometric condition). All the experiments were done at room temperature (20°C) except the relaxing ones using rabbit psoas bundles, when the temperature of the solution used before freezing was 28°C. Isometric contractions were also initiated from rigor by changing the bundles from the solution A to the contracting solution.

After plunging, the bundle remained attached to the lever and transducer arms and was recovered from the cryogen by grabbing it with a filter paper clamp placed at the tips of a self-closing pair of forceps. The forceps with the attached filter paper were precooled in liquid nitrogen. The filter paper with the bundle inside was then deposited into liquid nitrogen for storage until transfer to the freeze substitution medium.

Freeze substitution and electron-microscope procedures

The frozen bundles were freeze-substituted for at least 12 h in 4% tannic acid (Electron Microscope Sciences, Fort Washington, PA) in acetone at −80°C. After this period, the bundles in the freeze substitution media were taken out of the refrigeration and allowed to warm to room temperature (time ~50 min). The freeze substitution media was exchanged for acetone, and the bundles were post-fixed with 2% osmium tetroxide in acetone for 5 min at room temperature. Then, the bundles were block-stained for 2 h with 2% uranyl acetate in methanol or 0.5% uranyl acetate in acetone. We found that the use of either methanol or acetone gave good ultrastructural preservation, but the use of acetone gave specimens that showed much clearer layer lines in the 1/5.9 nm^{-1} region of the micrograph's optical diffraction patterns. After block-staining, the bundles were infiltrated with the plastic embedding medium. The bundles were placed in a 1:1 mixture of acetone and embedding medium for ~4 h and then overnight in the embedding medium. The bundles, in the uncured plastic, were then cut with a razor blade perpendicularly to the fibers long axis to produce smaller pieces that were placed into flat embedding molds (Electron Microscope Sciences). To avoid having the bundle pieces at the bottom of the mold, they were placed on top of a flat piece of precured embedding medium. This procedure ensures that in the thin sections produced from the blocks, the sample is away from the section edge, where breaks and folds are usually present. The components and proportions of the embedding mixture were as in Reedy et al. (1983): 10 g of Araldite 506 resin, 15 g of dodecenyl succinic anhydride (DDSA), and 2 g of DER 736 resin. As accelerator 1.8% v/v tris-dimethylaminomethyl phenol (DMP-30) or 3% v/v benzyldimethylamine (BDMA) was used (all components of the embedding mixture from Electron Microscope Sciences). Sections of about 70 nm thick were cut using a microtome (Ultracut E, Reichert-Jung, Hernalser Hauptstrasse, Austria) with a diamond knife. To avoid compression artifacts along the myofilament long axis, the sections used for filament length measurements were always cut with the knife edge parallel to the long fiber axis. Sections were collected on carbon-coated 400 mesh grids and stained successively for 30 min in 2% uranyl acetate in water and in Reynolds lead citrate solution (Reynolds, 1963). Electron micrographs were taken using a Phillips 301 electron microscope operated at 80 kV.

Filament measurements

For myofilament length measurements, micrographs were taken at a nominal magnification of 9100X. The measurements were made on prints with a final magnification of ~23000X or, alternatively, the negatives were digitized and measured in a computer display. Actin filaments were measured from the center of the Z line to the H-zone or, in very short sarcomeres, to the boundary between the double overlap and the overlap regions. At sarcomere lengths where the end of the actin filament would have been confused with the bare zone, actin filament measurements were omitted. The final magnification of each print or digitized image was estimated using the myosin axial repeat as an internal standard and using the period in micrographs of negatively stained tropomyosin paracrystals (period = 39.5 nm; Cohen and Longley, 1966) as an external standard. The myosin axial repeat was measured in the micrograph's optical diffraction patterns and, to obtain the magnification factor a value of 14.5 nm, was assumed for this repeat. The paracrystal micrographs were taken under similar conditions in the same session as the specimen ones. The height of the specimens in the microscope column was checked by monitoring the objective current necessary to bring the image to focus. Several paracrystal micrographs were taken in a range of current values similar to the specimen ones. From these micrographs the relationship between objective current and magnification was obtained. For a given value of objective current, the amount of variability in the measured paracrystal spacing was ~1%.

The optical diffraction patterns of the micrographs were surveyed and recorded using an optical diffractometer as described by Salmon and DeRosier (1981).

X-ray diffraction

For X-ray analysis the embedded muscle fibers were mounted on a thin piece of mica. The sample was then directly mounted on the last slit of the x-ray camera, which consisted of either a double mirror or a mirror-monochromator camera and a vacuum tube between the specimen and the film (Kodak, DEF 2). The x-ray source was a GX-13 rotating anode operated at 30 kV and 50 mA.

RESULTS

Ultrastructural preservation

After rapid freezing and freeze substitution, the frozen bundles did not appear mechanically distorted. At this stage in the procedure, the parts damaged by ice crystal formation could be recognized (before osmium fixation) by their opaque appearance. The bundles frozen with cryoprotection were translucent and showed interference colors, indicating good ultrastructural preservation. Electron micrographs of thin sections at various depth into the fiber bundle also revealed excellent ultrastructural preservation and absence of ice crystal damage. No noticeable ultrastructural differences, related to the tissue depth, were observed in the cryoprotected samples. The preservation of entire bundles up to 500 μm in diameter made it possible to obtain x-ray diffraction patterns from them after freeze substitution and embedding (Fig. 4). These patterns were used to assess the adequacy of different freeze substitution protocols before the thin sectioning step.

Without using cryoprotectants it was possible to obtain some areas at the bundle surface with good structural preservation, but ice crystal damage was observed in most parts of the bundle.

In the micrographs, the quality of the preservation could be assessed from the regularity and detail of the periodic structure visible in the actin and myosin filaments. Fig. 2 shows typical thin section (~70 nm thick) micrographs of muscle fiber bundles frozen in the rigor, contracting, and relaxing states. The actin and myosin periodicities showed up in these sections as a series of fine lines crossing the A and I bands. The preservation of these regular structures can be

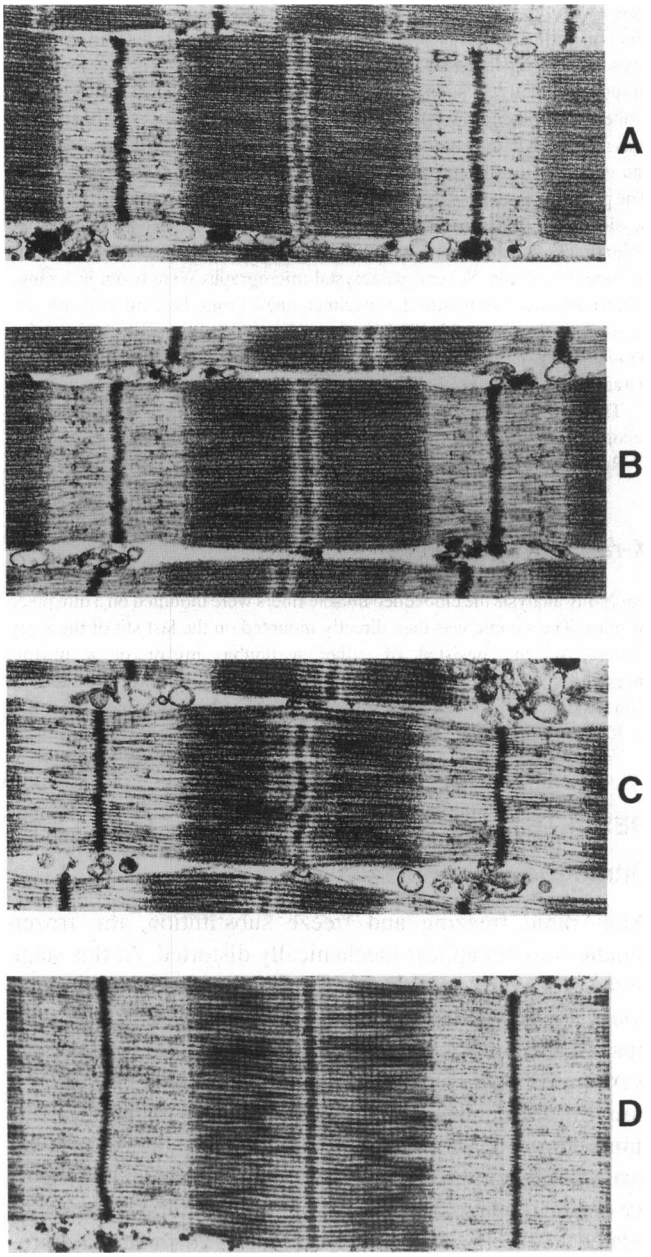

FIGURE 2 Thin section (~70 nm) micrographs of rapid frozen and freeze substituted muscle samples. Rigor rabbit muscle (*A*). Isometrically contracting rabbit muscle (*B*). Relaxed rabbit muscle (*C*). Relaxed frog muscle (*D*).

assessed more quantitatively from the presence of characteristics layer lines in the corresponding optical diffraction patterns (Fig. 3).

The optical diffraction patterns show layer lines with periodicities corresponding to the myosin and actin filaments up to at least the ~1/5.9 nm^{-1} actin layer line (Fig. 3). Higher order meridional layer lines are present in the x-ray patterns from the embedded bundles (Fig. 4). The layer lines have similar axial spacing and intensity profiles to those seen in the x-ray diagrams of unfixed muscles (Huxley and Brown, 1967). Moreover, the differences in intensity in the x-ray patterns associated with different physiological states of the muscle are reproduced in the optical diffraction patterns of muscle samples frozen in analogous conditions.

To aid in the comparison of the relative spacing and intensities on the optical diffraction patterns, the summed intensities along the layer lines are plotted in Fig. 5 for the three experimental conditions studied.

Rigor conditions

Optical diffraction patterns of micrographs of rabbit psoas muscle frozen in the absence of ATP (rigor condition) are characterized by strong actin-related layer lines (Fig. 3 *A*). The first actin layer line at 1/37.2 nm^{-1} is a dominant feature of the pattern, and the 6th at 1/5.9 nm^{-1} is also strong in comparison with the contracting or relaxed patterns. Also present is the second actin layer line at 1/18.6 nm^{-1} and some other weaker actin-related layer lines at 1/9.1 nm^{-1} (actin 4th order) and 1/7.2 nm^{-1} (actin 5th order). There are two layer lines that are characteristic of the rigor state at 1/23.7 nm^{-1} and 1/10.4 nm^{-1} (3d and 7th order of a ~72 nm repeat; see Huxley and Brown, 1967; Haselgrove, 1975). The troponin-related meridional layer line at 1/38.5 nm^{-1} is also present. The myosin-related meridional reflection at ~1/14.5 nm^{-1} is a strong feature on the rigor optical diffraction pattern, and there are other myosin meridionals at 1/42.9 nm^{-1} and 1/21.9 nm^{-1}.

Contracting conditions

Bundles were frozen in contracting solution (high Ca^{2+} and ATP) at the tension plateau of isometric contraction or during active shortening. The optical diffraction patterns from the sections of the isometrically contracting muscles (Fig. 3 *B*) show the ~1/14.5 nm^{-1} myosin meridional reflection and have very weak or absent off-meridional layer lines in the ~1/37 nm^{-1} (actin) region. There is a weak off-meridional layer line at 1/42.9 (myosin) nm^{-1}. At 1/38.5 nm^{-1} (troponin), there is a layer line with maximum at the meridian but that spreads off-meridionally. The 1/5.9 nm^{-1} (actin) was weaker than in the rigor condition but clearer than in the relaxing case. The optical diffraction patterns of actively shortening bundles were similar to the isometric ones, but we have not fully analyzed possible differences between them yet.

Relaxing conditions

When rabbit psoas fiber bundles were fixed in the presence of ATP but no Ca^{2+} (relaxing conditions), the electron micrographs show less periodic structure than was visible in the rigor micrographs (Fig. 2 *C*). The corresponding optical diffraction patterns show a relatively large amount of low angle continuous scattering (Fig. 3 *C*), suggesting some disorder of the myosin heads, but layer lines at several order of the 42.9 nm myosin related repeat, as expected for a striated muscle at rest (Huxley and Brown 1967), are present (Figs. 3 *C* and 5). The 1/5.9 nm^{-1} actin layer line was also visible but was much weaker than in the rigor patterns (Figs. 3 *C* and 5).

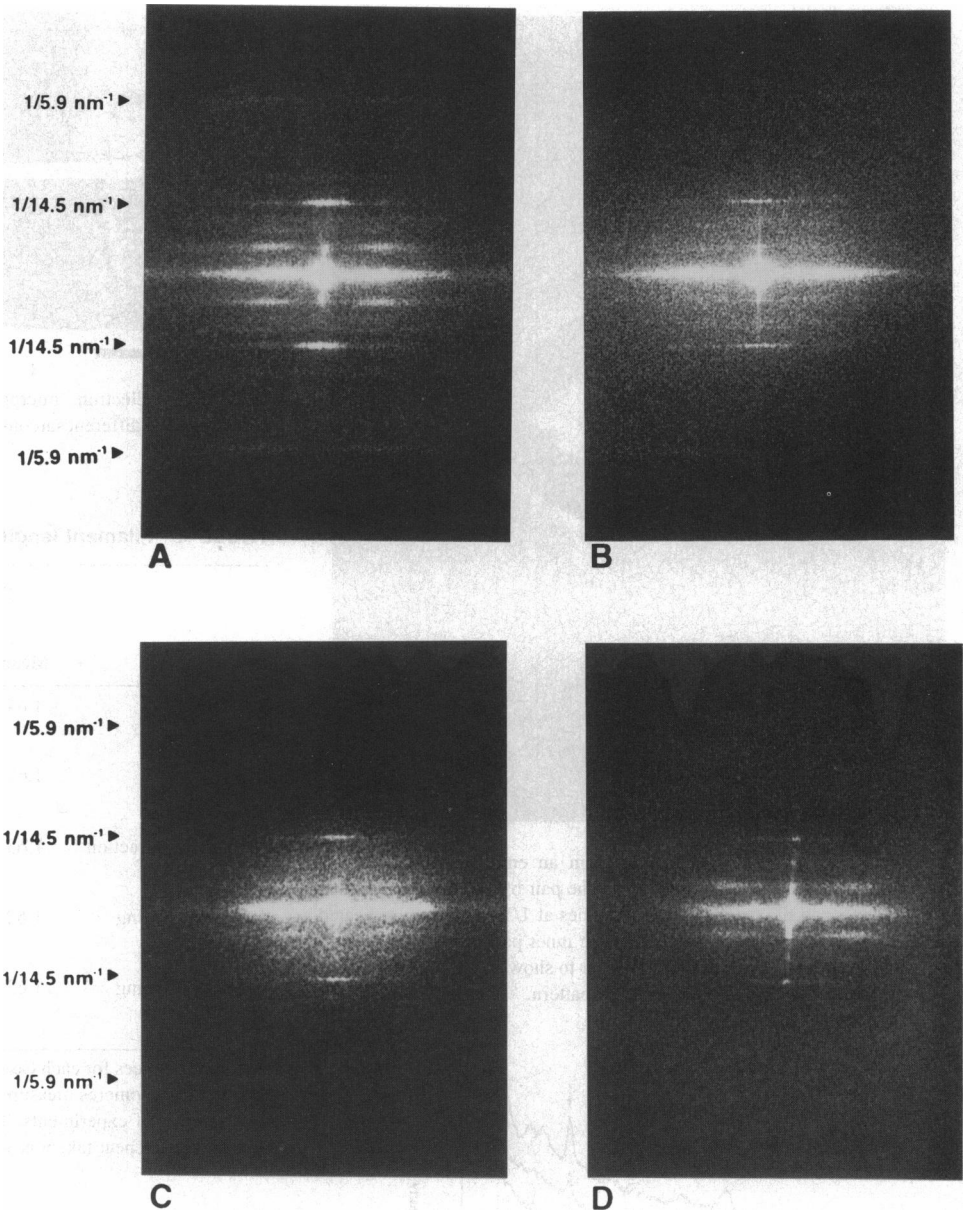

FIGURE 3 Optical diffraction patterns corresponding to Fig. 2 micrographs. Rigor rabbit muscle (*A*). Isometrically contracting rabbit muscle (*B*). Relaxed rabbit muscle (*C*). Relaxed frog muscle (*D*). The 1/14.5 and 1/5.9 nm^{-1} reciprocal spacings are indicated.

We also obtained micrographs and optical diffraction patterns of frog (semitendinosus) muscles, because the resting thick filament structure in rabbit is known to be very sensitive to temperature and ionic conditions (Wray, 1987; Wakabayashi et al., 1988; Rinne and Wray, 1990), and it was conceivable that the rabbit pattern was affected by some evaporation of solution and/or cooling taking place between the time that the bundle was withdrawn from the bulk of the solution and was immersed into the cryogen. Indeed, we found that the myosin layer lines were more intense in the optical diffraction patterns from micrographs of frog muscles in relaxing conditions (Fig. 3 *D*).

Filament lengths

The length of the filaments was measured in conditions of relaxation, rigor, isometric contraction, and active shortening in micrographs similar to the ones shown in Figs. 2 and 6. The active shortening measurements were separated in two groups based on the amount of tension measured at the moment of freezing in relation to the maximum isometric tension of the bundle (P_o).

On average, the lengths of the myosin and actin filaments are 1.63 and 1.12, μm respectively (Table 1 and Fig. 7). The maximum difference observed between the mean values was 3.5% of the filament length in the case of the actin filament (1.11 vs. 1.15 μm) and 1.2% in the case of the myosin filament (1.62 vs. 1.65 μm). These differences are of doubtful significance because they are in the range of the experimental error of the measurements (0.02–0.05 μm). Some variability in the measurements is expected due to the difficulty in defining the end of the filaments precisely. In addition, axial distortions (e.g., shrinkage) produced by the preparative procedures and residual magnification errors may also contribute to this variability.

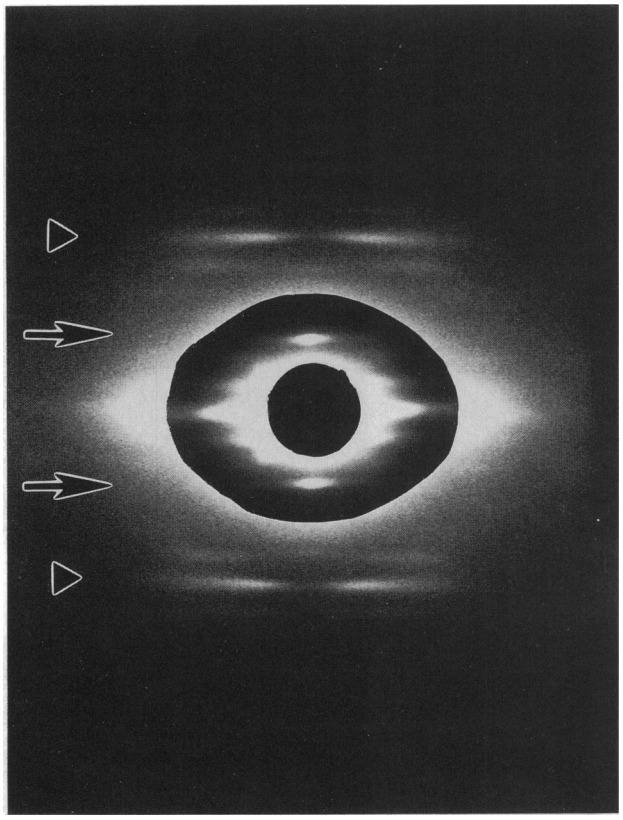

FIGURE 4 X-ray diffraction pattern from an embedded muscle fiber bundle plunge frozen in rigor conditions. The pair of myosin layer lines at ~1/14.5 nm^{-1} and the pair of actin layer lines at 1/5.9 nm^{-1} are indicated with arrows and triangles, respectively. The inner part of this pattern is at a lower exposure than the outer part in order to show in a single picture the higher and lower intensity features of the pattern.

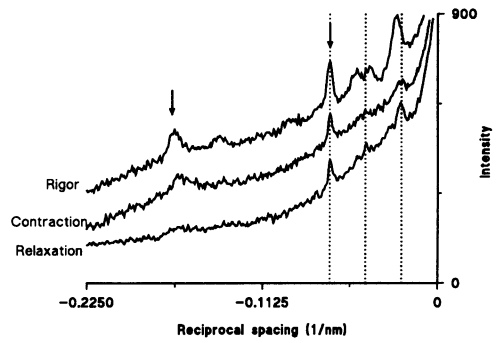

FIGURE 5 Densitometric traces from optical diffraction patterns corresponding to rigor, contracting and relaxed frozen rabbit muscles. The traces correspond to the projected intensity along layer lines. The optical diffraction patterns correspond to an area in the electron micrograph containing one sarcomere. Arrows indicate the 1/14.5 nm^{-1} (*rightmost arrow*) and 1/5.9 nm^{-1} (*leftmost arrow*) spacings. The traces are displaced vertically with respect to each other to avoid superposition. The three vertical dotted lines indicate myosin spacings at 1/43.5, 1/21.8, and 1/14.5 nm^{-1}. No attempt was made to normalize the intensities between the three optical diffraction patterns, although they were obtained in similar conditions in the three cases.

During contraction, the myofilament lengths remain constant independently of the sarcomere length (Fig. 8) or the amount of sarcomere length change (Fig. 9). Data for elongated sarcomeres came from some active shortening experiments (Note in Fig. 9 that there are sarcomeres that increase in length during contraction) in which inhomogeneous length changes resulted in shortened and elongated sarcomeres. As shown in Fig. 9, the filament length in these elongated sarcomeres is also similar to the isometric or shortened sarcomeres.

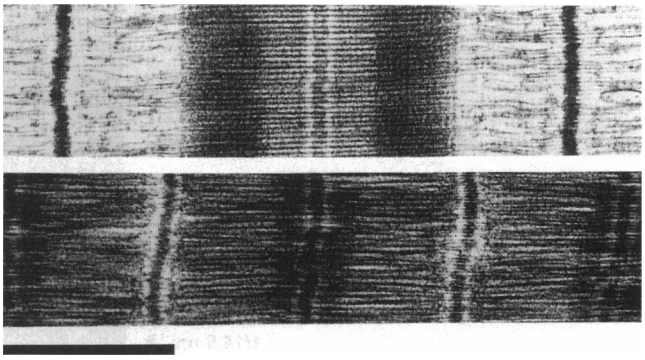

FIGURE 6 Electron micrographs from rapidly frozen contracting muscles at two different sarcomere lengths. The calibration bar at the bottom is 1 μm long.

TABLE 1 Filament length in each experimental condition

	Thick filament length μ			Thin filament length μ		
	Mean	SD	*n*	Mean	SD	*n*
Relaxation	1.64	0.04	122	1.11	0.03	73
			14			9
			3			3
Rigor	1.62	0.03	136	1.11	0.02	46
			17			8
			4			2
Isometric contraction	1.63	0.02	160	1.15	0.02	50
			9			8
			4			2
Active shortening	1.62	0.05	321	1.13	0.03	173
			35			22
(0–20% P_o)			9			9
Active shortening	1.63	0.03	326	1.12	0.02	147
			34			16
(30–50% P_o)			6			5

The three *n* values for each case correspond, from top to bottom, to the total number of sarcomeres measured, the total number of micrographs, and the total number of experiments. The length values are calibrated against the myosin axial repeat taken as 14.5 nm. SD, standard deviation.

The length values in Table 1 and Figs. 7–9 were calculated using the myosin axial period as an internal standard in each micrograph. The use of an external standard (tropomyosin paracrystal) gave similar values, and constancy of filament lengths was also observed, independent of the sarcomere length or its changes. Thus, the possibility of a genuine length change being masked by a corresponding change in the myosin axial repeat is ruled out. The myosin spacing in the micrographs calculated against the external standard was 14.22 ± 0.16 nm (n = 9) close to the myosin axial spacing measured by x-ray diffraction (14.34 nm in rest frog muscle and ~1% longer during contraction; Huxley and Brown,

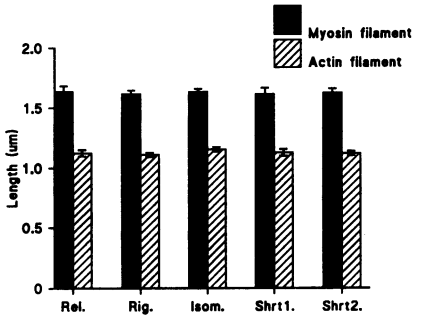

FIGURE 7 Filaments length in each experimental condition. Rel: Relaxing conditions. Rig: Rigor conditions. Isom: Isometric conditions. Shrt1: Active shortening, tension = 0–20% P_0 at freezing time. Shrt2: Active shortening, tension = 30–50% P_0 at freezing time.

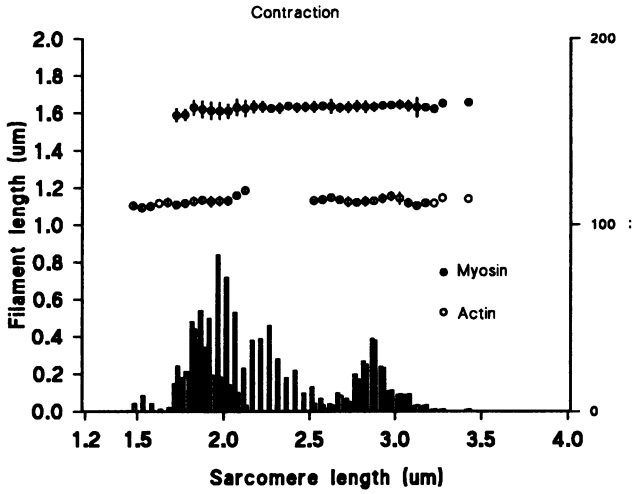

FIGURE 8 Filament length versus sarcomere length. n is the number of sarcomeres measured. Circles indicate the average filament length (●, myosin; ○, actin), and the vertical lines indicate SD. The bars represent the number of sarcomeres measured (*filled*, myosin; *open*, actin). The measurements were grouped into sarcomere length intervals of 0.05 μm.

1967; Haselgrove, 1975). The troponin repeat in the I-band gave a value of 39.06 ± 0.95 nm (n = 11), similar to the reported value in x-ray diffraction studies (~38.5 nm; Huxley and Brown, 1967; Rome et al., 1973). The similarity of spacing indicates little alterations of the specimen dimensions in the procedure. We notice, however, when comparing the myosin axial spacing in the overlap and in the non-overlap region in stretched sarcomeres, that the spacing in the overlap region is slightly smaller, typically <2% smaller, but cases with bigger differences were observed. We found this difference in specimens frozen in contracting, relaxing, or rigor conditions.

DISCUSSION

Plunge freezing and freeze substitution method

We have developed a rapid freezing and freeze substitution method that produces extremely well preserved muscle specimens for electron microscope observation. We rapidly

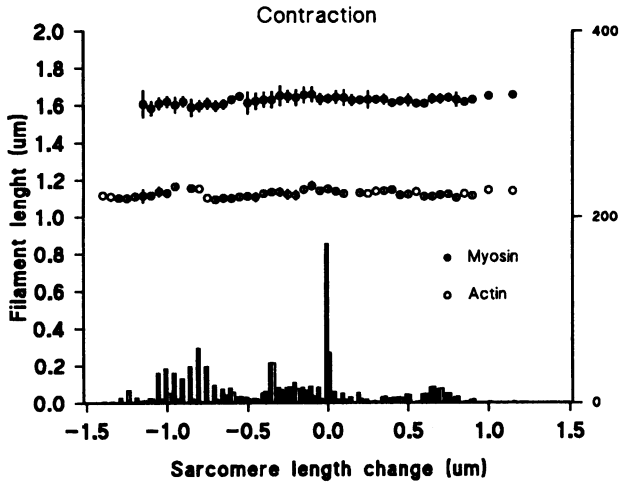

FIGURE 9 Filament length versus amount of sarcomere shortening during contraction. Final sarcomere length was measured in the micrographs and initial sarcomere length was measured in the fiber bundles by laser diffraction before contraction. Symbol convention as in Fig. 8. Measurement grouped in sarcomere length difference intervals of 0.05 μm.

froze the samples by plunging them into a liquid cryogen. When uncryoprotected samples are frozen against a cold metal block (e.g., Heuser et al., 1979; Tsukita and Yano, 1985; Padrón et al., 1988; Hirose et al., 1993), even at liquid helium temperatures, only a layer of a few microns is well preserved; the rest of the sample shows ice crystal damage. Use of cryoprotectant extends the depth of good preservation (Huxley, 1987 and unpublished results), but considerable variation in freezing quality still prevails, and the fibers are also generally deformed in the slamming procedure. We found that with the use of the plunging method, flattening of the fibers and ultrastructural mechanical distortions is avoided, and when cryoprotection is used, ice crystal damage is also avoided throughout the entire fiber bundle. As a result, it is possible to obtain x-ray diffraction patterns of the entire fiber bundle after embedding, which enables one to evaluate the quality of the specimens before the sectioning step.

In our system, without using cryoprotectants, we obtained areas without ice damage 2–5 μ deep, although most parts of the bundles were not well preserved. For this reason, we used cryoprotection in our experiments. To obtain more areas devoid of ice damage, it is possible to improve the cooling rate of our system by increasing the plunging speed currently at 2.3 m/s (see Handley, 1981; Elder et al., 1982; Robard and Sleytr, 1985; Ryan and Purse, 1985). Regarding the use of other cryogens, we used ethane because it has been reported to have the fastest cooling rate with bare thermocouples or with hydrated specimens (Ryan et al., 1987). But it is likely that other cryogens like propane would also give good results (in comparison with ethane, propane has a lower melting temperature and a higher boiling point but slightly lower specific heat and thermal conductivity at the melting point; see Robards and Sleytr, 1985).

The ability of our method to preserve the muscle ultrastructure is indicated by the fact that the x-ray patterns of the

embedded bundles and the optical diffraction patterns of the micrographs are comparable with x-ray patterns of unfixed specimens in similar states. The preparations give a rigor pattern with strong actin-related layer lines, a relaxed pattern dominated by myosin related layer lines and a contracting pattern that shows weak off meridional actin or myosin layer lines but with a strong ~1/14.5 nm^{-1} myosin-related meridional reflection (Haselgrove, 1983; Huxley and Brown, 1967; Huxley et al., 1980). The intensity of the 1/5.9 nm^{-1} actin-related layer line in the optical diffraction patterns followed the relationship rigor > contraction > relaxation. This relationship is also in agreement with reported x-ray results (Huxley and Brown, 1967; Vibert et al., 1972; Haselgrove, 1975; Matsubara et al., 1984; Kress et al., 1986; Maeda et al., 1988; Wakabayashi et al., 1991).

The fact that the optical diffraction pattern of an area consisting of one or two sarcomeres shows clear layer lines in the 1/5.9 nm^{-1} region represents a significant improvement in the ultrastructural preservation of vertebrate striated muscle for electron microscopy. This improved preservation can be attributed, in part, to the use of tannic acid. Insect flight muscles chemically fixed in rigor with a mixture of glutaraldehyde and tannic acid show the actin layer lines at 1/5.9 and 1/5.1 nm^{-1} (Reedy and Reedy, 1985). Using a freeze substitution protocol including the use of tannic acid, Craig et al. (1992) reported layer lines at this resolution in some of the optical diffraction patterns of rapidly frozen frog muscles in rigor. By averaging many optical diffraction patterns to increase the signal to noise ratio, the 1/5.9 nm^{-1} layer line has also been reported in slam frozen rigor rabbit psoas specimens freeze substituted with osmium (Hirose et al., 1993). It was not clear, however, in these patterns if the layer line was meridional or off-meridional. With our procedure, we observe the off-meridional layer line at 1/5.9 nm^{-1} in virtually all of the optical diffraction patterns, especially in those corresponding to the rigor conditions. We found that in addition to the use of tannic acid, the use of acetone as the solvent in the freeze substitution and all subsequent steps greatly improves the preservation of layer lines at this resolution. Preservation of structural detail to even higher resolution was indicated by the presence of meridional layer lines beyond the 1/5.9 nm^{-1} in the x-ray patterns of the embedded bundles.

The similarity of the myosin and troponin axial periodicities measured in the micrographs to those measured by x-ray diffraction in intact muscle indicates little alteration in the specimen dimensions in contrast to some chemical fixation protocols where changes of the order of 10% have been reported (Page and Huxley, 1963). However, we noticed a different myosin spacing in the overlap and non-overlap regions. A similar finding has been reported using a chemical fixation protocol (Brown and Hill, 1982). We do not have a clear explanation for this behavior yet, but it is unlikely that this phenomenon is related to the force generating mechanism, because the difference in spacing is observed in relaxed fibers as well as rigor or contracting ones. Moreover, in x-ray diffraction studies on living muscles, no evidence has been found for mixed periodicities of the kind expected if the overlap and non-overlap region had the different axial periods seen in the micrographs (H. E. Huxley, unpublished observations).

Freezing time

In freezing experiments, it has been estimated that the outer 10 μm of the sample can be frozen in 2 ms or less (Heuser et al., 1979). The time resolution of the freezing methods is determined by the cooling rate and the temperature in which the structure of interest is immobilized. The cooling rate depends on many factors such as freezing method, size of the sample, and tissue depth. In several freezing systems, the cooling rates of hydrated specimens have been estimated using small thermocouples inside the specimen. Some reported values for plunging systems are ~2300 K/s with a specimen 120 μm thick (plunging into propane at ~2 m/s (see Escaig, 1982) or plunging into ethane at 2.3 m/s (see Ryan et al., 1987)) and 31000 K/s with a specimen 20 μm thick (Escaig, 1982). These values can be taken only as an approximation because they depend on the particular experimental conditions used, and the thermocouple itself affects the measurements. Theoretical analysis indicates that under optimal conditions the cooling rate in the outermost 10 μ of tissue is 10^6 K/s or higher (see Knoll et al., 1987).

Regarding the temperature in which immobilization occurs, x-ray crystallography and other physicochemical techniques have indicated a transition in the dynamic properties of proteins at 220 K (Rasmussen et al., 1992; Tilton et al., 1992). Studies on the enzyme ribonuclease-A have shown that below this temperature the substrate or an inhibitor cannot bind to the enzyme or, if already bound, they cannot dissociate. These results indicate that below 220 K, the conformational changes necessary for binding and dissociation at the active site are suppressed (Rasmussen et al., 1992). Thus, taking 220 K as the required temperature to stop conformational changes, with the aforementioned cooling rates, the time resolution of the freezing method (starting freezing at 293 K) will range from 73 μs (theoretical rate = 10^6 K/s) to 2.3 ms (small specimen rate = 31000 K/s) or 32 ms (large specimen rate = 2300 K/s). The freezing point of water (273 K) would be reached in about one-third of these times. This calculation assumes a constant cooling rate through the whole temperature interval. Note also that the target temperature (220 K) is higher than the temperature in which the freeze substitution process is performed (193 K). Thus, the substitution process is, in principle, done at a "safe" temperature in the sense that protein conformational changes should be suppressed.

Myofilament length

The main conclusion to be drawn from our filament measurements is that within experimental error (~0.03 μm), the length of both actin and myosin filaments is the same in the relaxed, rigor, and contracting states. It also remains the same

when the muscle actively shortens to sarcomere lengths below the resting length (~2.2 μm). This study confirms with much higher accuracy the early optical microscope studies that showed no change in A-band and I-filament length at sarcomere lengths at or above the resting length (Huxley and Niedegerke 1954, 1958; Huxley and Hanson, 1954), which provided much of the basis for the sliding filament mechanism. It adds new evidence that during contraction at sarcomere lengths below the in situ length (~2.2 μm), the filament dimensions also remain constant and that no changes occur during active shortening.

As suggested by Huxley and Niedegerke (1958), limits in the resolution of optical systems might be the cause of the apparent filament shortening observed below resting lengths by optical microscopy. A variety of other artifacts, which have been discussed by Page and Huxley (1963) and by Huxley (1985), might have been the cause of misleading electron microscope observations. This work supports previous electron microscope observations, where constancy of filaments length during contraction was observed (Page and Huxley, 1963) and the use of rapid freezing relieves the concerns derived from the slow fixation time of the chemical fixation methods used in such studies.

Our conclusions about the filament lengths are in disagreement with a recent study reporting up to a 50% decrease in the thick filament length during active shortening as measured by optical microscopy or a ~19% decrease as measured by electron microscopy in chemically fixed muscles (Periasamy et al., 1990). In the case of the optical microscope study, we believe the discrepancy with our results is still due to the lower resolution of optical microscopy. This is indicated by the lack of a density transition at the boundary between the A and I bands in the densitometric traces from the optical microscope records in the cited work. In the case of the electron microscope results, the origin of the discrepancy with our results is not clear, but artifacts caused by the chemical protocol used are conceivable. We believe, based on the ultrastructural preservation already discussed, that rapid freezing and freeze substitution gives a more faithful representation of the muscle ultrastructure during contraction.

Our results show no indication whatsoever that the filament sliding process in contraction is produced by or accompanied by changes in filament length in any condition. Thus, the results argue strongly against proposals of thick and/or thin filament shortening as either the responsible mechanism or a secondary phenomenon in muscle contraction (e.g., Pollack 1990; Schutt and Lindberg, 1992).

It is important to point out that, in this work, when we conclude that the myofilaments remain at a constant length, it means no changes bigger than ~3.5% of the filament length (maximum difference observed between filaments mean values). Changes in spacing smaller than this would be difficult to detect by electron microscopy. It is known from x-ray diffraction studies that the myosin axial spacing increases by about 1% when going from rest to contraction (Huxley and Brown, 1967; Haselgrove, 1975). The nature of this spacing increase and of any other possible small length changes in the myofilaments is currently being investigated by x-ray diffraction (Huxley et al., 1994).

Future prospects

We have developed a rapid freezing and freeze substitution procedure that gives improved ultrastructural preservation of the myofilaments in static and dynamic states, showing detail at least up to 1/5.9 nm^{-1}. This resolution is adequate to observe possible structural changes in the cross-bridges, which are thought to exert elementary power strokes of 4–12 nm (Huxley and Simmons, 1971; Huxley and Kress, 1985). Micrographs of muscle samples frozen in different mechanical conditions should make it possible to detect structural changes correlated with the force producing mechanism. With this goal, we have frozen contracting muscle fibers in different mechanical conditions including very fast length transients, and we are now analyzing ultrathin sections where individual cross-bridges are discernible.

We thank Dr. Alex Stewart for discussions and help with the computers, Dr. M. K. Reedy for discussions, Charles Ingersoll for building the plunger, Barkev Bablouzian for help building some electronic devices, and Marie Craig for photographic work.

This work was supported by National Institutes of Health grant ARE38899, by a NATO postdoctoral fellowship from Deutscher Akademisches Austanschdienst (DAAD) (D. Popp), and by a grant from the Lucille P. Markey Charitable Trust (H. E. Huxley).

REFERENCES

Bald, W. B. 1985. The relative merits of various cooling methods. *J. Microscopy.* 140:17–40.

Brown, L. M., and L. Hill. 1982. Mercuric chloride in alcohol and chloroform used as a rapidly acting fixative for contracting muscle fibers. *J. Microscopy.* 125:319–336.

Cohen, C., and W. Longley. 1966. Tropomyosin paracrystals formed by divalent cations. *Science.* 152:794–796.

Craig, R., L. Alamo, and R. Padrón. 1992. Structure of the myosin filaments of relaxed and rigor vertebrate striated muscle studied by rapid freezing electron microscopy. *J. Mol. Biol.* 228:474–487.

De Villafranca, G. W. 1961. The A and I band lengths in stretched or contracted horseshoe crab skeletal muscle. *J. Ultrastruct. Res.* 5:109–115.

Dewey, M. M., R. J. C. Levine, and D. E. Colflesh. 1973. Structure of *Limulus* striated muscle. *J. Cell Biol.* 58:574–598.

Eastwood, A. B., D. S. Wood, K. L. Bock, and M. M. Sorenson. 1979. Chemically skinned mammalian skeletal muscle. I. The structure of skinned rabbit psoas. *Tissue and Cell.* 11:553–566.

Elder, H. Y., C. C. Gray, A. G. Jardine, J. N. Chapman, and W. H. Biddlecombe. 1982. Optimum conditions for cryoquenching of small tissue blocks in liquid coolants. *J. Microscopy.* 126:45–61.

Escaig, J. 1982. New instruments which facilitate rapid freezing at 83 K and 6 K. *J. Microscopy.* 126:221–229.

Handley, D. A., J. T. Alexander, and S. Chien. 1981. The design and use of a simple device for rapid-quench-freezing of biological samples. *J. Microscopy.* 121:273–282.

Haselgrove, J. C. 1975. X-ray evidence for conformational changes in the myosin filaments of vertebrate striated muscle. *J. Mol Biol.* 92:113–143.

Haselgrove, J. C. 1983. Structure of vertebrate striated muscle as determined by x-ray diffraction studies. *In* Handbook of Physiology. L. D. Peachey, editor. American Physiological Society. Williams & Wilkins, Baltimore. 143–171.

Heuser, J. E., T. S. Reese, M. J. Dennis, Y. Jan, L. Jan, and L. Evans. 1979. Synaptic vesicle exocytosis captured by quick freezing and correlated with quantal transmitter release. *J. Cell Biol.* 81:275–300.

Hirose, K., T. D. Lenart, J. M. Murray, C. Franzini-Armstrong, and Y. Goldman. 1993. Flash and smash: rapid freezing of muscle fibers activated by photolysis of caged ATP. *Biophys. J.* 65:397–408.

Hirose, K., and T. Wakabayashi. 1988. Thin filaments of rabbit skeletal muscle are in helical register. *J. Mol. Biol.* 204:797–801.

Huxley, A. F., and R. Niedergerke. 1954. Structural changes in muscle during contraction. *Nature.* 173:971–973.

Huxley, A. F., and R. Niedergerke. 1958. Measurement of the striations of isolated muscle fibers with the interference microscope. *J. Physiol.* 144: 403–425.

Huxley, A. F., and R. M. Simmons. 1971. Proposed mechanism of force generation in striated muscle. *Nature.* 233:533–538.

Huxley, H. E. 1985. The crossbridge mechanism of muscular contraction and its implications. *J. Exp. Biol.* 115:17–30.

Huxley H. E. 1987. Correlation between X-ray diffraction studies on contracting muscle and electron microscope observations using rapid freezing techniques. *Biophys. J.* 51:5*a*. (Abstr.)

Huxley, H. E., and W. Brown. 1967. The low angle X-ray diagram of vertebrate skeletal muscle and its behavior during contraction and rigor. *J. Mol. Biol.* 30:383–343.

Huxley, H. E., A. R. Faruqi, J. Bordas, M. H. J. Koch, and J. R. Milch. 1980. The use of synchrotron radiation in time-resolved X-ray diffraction studies of myosin layer-lines reflections during muscle contraction. *Nature.* 284:140–143.

Huxley, H. E., and J. Hanson. 1954. Changes in the cross-striations of muscle during contraction and stretch and their structural interpretation. *Nature.* 173:973–976.

Huxley, H. E., and M. Kress. 1985. Crossbridge behaviour during muscle contraction. *J. Musc. Res. Cell Motil.* 6:153–161.

Huxley, H. E., A. Stewart, H. Sosa, and T. Irving. 1994. X-ray diffraction measurements of the extensibility of the actin and myosin filaments in muscle. *Biophys. J.* 66:191*a* (Abstr.)

Jones, G. H. 1984. On estimating freezing times during tissue rapid freezing. *J. Microscopy.* 136:349–360.

Knoll, G., A. J. Verkleij, and H. Plattner. 1987. Cryofixation of dynamic processes in cell and organelles. *In* Cryotechniques in Biological Electron Microscopy. R. A. Steinbrecht and K. Zierold, editors. Springer-Verlag, Berlin. 258–271.

Kress, M., H. E. Huxley, A. R. Faruqi, and J. Hendrix. 1986. Structural changes during activation of frog muscle studied by time resolved X-ray diffraction. *J. Mol. Biol.* 188:325–342.

Levine, R. J. C, J. L. Woodhead, and H. A. King. 1991. The effect of calcium activation of skinned fiber bundles on the structure of *Limulus* thick filaments. *J. Cell Biol.* 113:573–583.

Maeda, Y., D. Popp, and S. M. MacLaughlin. 1988. Cause of changes in the thin filament-associated reflexions on activation of frog muscle. Myosin binding or conformational change of actin. *In* Molecular Mechanism of Muscle Contraction. H. Sugi and G. H. Pollack, editors. Plenum Press, New York. 381–390.

Matsubara, I., N. Yagi, H. Miura, M. Ozeki, and T. Izumi. 1984. Intensification of the 5.9 nm actin layer line in contracting muscle. *Nature.* 255:728–729.

McDowall, A. W., W. Hofman, J. Lepault, M. Adrian, and J. Dubochet. 1984. Cryo-electron microscopy of vitrified insect flight muscle. *J. Mol. Biol.* 178:105–111.

Moisescu, D. G. 1976. Kinetics of reaction in calcium-activated skinned muscle fibers. *Nature.* 262:610–613.

Moor, H. 1971. Recent progress in the freeze-etching technique. *Phil. Trans. R. Soc. Ser. B.* 261:121–131.

Padrón, R., L. Alamo, R. Craig, and C. Caputo. 1988. A method for quick-freezing live muscles at known instants during contraction with simultaneous recording of mechanical tension. *J. Microscopy.* 151:81–102.

Padrón, R., and R. Craig. 1989. Disorder induced in nonoverlap myosin cross-bridges by loss of adenosine triphosphate. *Biophys. J.* 56:927–933.

Padrón, R., M. Granados, L. Alamo, J. R. Guerrero, and R. Craig. 1992. Visualization of myosin helices in sections of rapidly frozen relaxed tarantula muscle. *J. Struct. Biol.* 108:269–276.

Page, S. G., and H. E. Huxley. 1963. Filaments lengths in striated muscle. *J. Cell Biol.* 19:369–390.

Periasamy, A., D. H. Burns, D. N. Holdren, G. H. Pollack, and K. Trombitas. 1990. A-band shortening in single fibers of frog skeletal muscle. *Biophys. J.* 57:815–828.

Pollack, G. H. 1983. The cross-bridge theory. *Physiol. Rev.* 63:1049–1113.

Pollack, G. H. 1990. Muscles and Molecules. Uncovering the Principles of Biological Motion. Ebner & Sons publishers, Seattle.

Rasmussen, B. J., A. M. Stock, D. Ringe, and G. A. Petsko. 1992. Crystalline ribonuclease A loses function below the dynamical transition at 220 K. *Nature.* 357:423–424.

Reedy, M. K., R. S. Goody, W. Hofmann, and G. Rosenbaum. 1983. Coordinated electron microscopy and X-ray studies of glycerinated insect flight muscle. I. X-ray diffraction monitoring during preparation for electron microscopy of muscle fibres fixed in rigor, in ATP and in AMPPNP. *J. Muscle Res. Cell Motil.* 4:25–53.

Reedy, M. K., and M. C. Reedy. 1985. Rigor crossbridge structure in tilted single filament layers and flared-X formations from insect flight muscle. *J. Mol. Biol.* 185:145–176.

Reynolds, E. S. 1963. The use of lead citrate at high pH as an electron-opaque stain in electron microscopy. *J. Cell Biol.* 17:208–212.

Rinne, B., and J. S. Wray. 1990. Effect of ionic conditions on the cross-bridge array in relaxed rabbit muscle. *J. Muscle Res. Cell Motil.* 11:67*a* (Abstr.)

Robards, A. W., P. W. Murray, and P. R. Waites. 1988. Countercurrent plunging: improved reproducibility of ultra-rapid cooling. *In* Proceedings of the 9th European Congress on Electron Microscopy. Institute of Physics Conference Series. No. 93, Vol. 3, Chapter 2. EUREM 88, York, England.

Robards, A. W., and U. B. Sleytr. 1985. Low Temperature Methods in Biological Electron Microscopy. Elsevier Science Publishers, Amsterdam. 551 pp.

Rome, E. M., T. Hirabayashi, and S. V. Perry. 1973. X-ray diffraction of muscle labelled with antibody to troponin-C. *Nature.* 244:154–155.

Ryan, K. P., and D. H. Purse. 1985. Plunge-cooling of tissue blocks: determinants of cooling rates. *J. Microscopy.* 140:47–54.

Ryan, K. P., D. H. Purse, S. G. Robinson, and J. W. Wood. 1987. The relative efficiency of cryogens used for plunge-cooling biological specimens. *J. Microscopy.* 145:89–96.

Salmon, E. D., and D. DeRosier. 1981. A surveying optical diffractometer. *J. Microscopy.* 123:239–247.

Sosa, H., D. Popp, G. Ouyang, and H. E. Huxley. 1992. Study of filaments lengths during contraction by electron microscopy of quick frozen muscle fibers. *Biophys. J.* 61:300*a*. (Abstr.)

Schutt, C. E., and U. Lindberg. 1992. Actin as the generator of tension during muscle contraction. *Proc. Natl. Acad. Sci. USA.* 89:319–323.

Tilton, R. F. Jr., J. C. Dewan, and G. A. Petsko. 1992. Effects of temperature on protein structure and dynamics: X-ray crystallographic studies of the protein ribonuclease-A at nine different temperatures from 98 to 320 K. *Biochemistry.* 31:2469–2481.

Trus, B. L., A. C. Steven, A. W. MacDowall, M. Unser, J. Dubochet, and R. J. Podolsky. 1989. Interactions between actin and myosin filaments in skeletal muscle visualized in frozen-hydrated thin sections. *Biophys. J.* 55:713–724.

Tsukita, S., and M. Yano. 1985. Actomyosin structure in contracting muscle detected by rapid freezing. *Nature.* 317:182–184.

Van Harreveld, A., J. Trubatch, and J. Steiner. 1974. Rapid freezing and electron microscopy for the arrest of physiological processes. *J. Microscopy.* 100:189–198.

Vibert, P. J., J. C. Haselgrove, J. Lowy, and F. R. Poulsen. 1972. Structural changes in actin-containing filaments of muscle. *J. Mol. Biol.* 71:757–767.

Wakabayashi, T., T. Akiba, K. Hirose, A. Tomioka, M. Tokunaga, C. Suzuki, K. Toyoshima, K. Sutoh, K. Yamamoto, T. Matsumoto, K. Sacki, and Y. Ameyima. 1988. Temperature induced changes of thick filaments and location of the functional site of myosin. *In* Molecular Mechanism of Muscle Contraction. H. Sugi and G. H. Pollack, editors. Plenum Publishing Corp., New York. 39–48.

Wakabayashi, K., H. Tanaka, H. Saito, N. Moriwaki, Y. Ueno, and Y. Ameyima. 1991. Dynamic X-ray diffraction of skeletal muscle contraction: structural change of actin filaments. *Adv. Biophys.* 27:3–13.

Wray, J. S. 1987. Structure of relaxed myosin filaments in relation to nucleotide state in vertebrate skeletal muscle. *J. Muscle Res. Cell Motil.* 8:62*a*. (Abstr.)